

# Stable Rh<sub>2</sub>(MTPA)<sub>4</sub> Phosphane Adducts – The First Example of *P*-Chirality Recognition by <sup>103</sup>Rh NMR Spectroscopy

Damian Magiera,<sup>[a]</sup> Wolfgang Baumann,<sup>[b]</sup> Ivan S. Podkorytov,<sup>[c]</sup> Jan Omelanczuk,<sup>[d]</sup> and Helmut Duddeck<sup>\*[a]</sup>

**Keywords:** Phosphanes / Rhodium / NMR spectroscopy / Chirality / Chiral discrimination

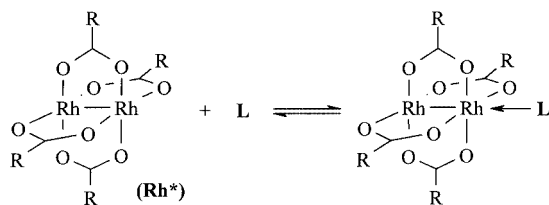
The optimal parameters for <sup>31</sup>P-detected <sup>103</sup>Rh HMQC NMR spectroscopy of AMX spin systems (A = <sup>31</sup>P; M and X = <sup>103</sup>Rh) have been derived and applied to adducts of Rh<sub>2</sub>[(*R*)-MTPA]<sub>4</sub> with PPh<sub>3</sub> (**1**) and a chiral phosphane (**2**). It is shown that all

nuclei (<sup>1</sup>H, <sup>13</sup>C, <sup>31</sup>P, and <sup>103</sup>Rh) reflect the diastereomerism of the latter complex.

(© Wiley-VCH Verlag GmbH, 69451 Weinheim, Germany, 2002)

## Introduction

In a series of papers<sup>[1]</sup> we have studied the potential of the dirhodium complex Rh<sub>2</sub>[(*R*)-MTPA]<sub>4</sub> (**Rh\***; MTPA-H = methoxytrifluoromethylphenylacetic acid, Mosher's acid) as a chiral solvating agent for the chiral recognition of various chiral monofunctional ligands **L**, i.e. for the determination of enantiomeric ratios.<sup>[2]</sup> We have shown that our “dirhodium method” is particularly suitable for soft-base functionalities where the classical method of chiral lanthanide-shift reagents (CLSR)<sup>[3]</sup> usually fails. Typically, **Rh\*** and **L** form kinetically labile adducts so that only averaged NMR signals can be observed (in analogy to the CLSR method) for the **L** molecules in equilibria as depicted in Scheme 1.



Scheme 1. Structure of Rh<sub>2</sub>[(*R*)-MTPA]<sub>4</sub> (**Rh\***) and schematic representation of adduct formation with a ligand **L**

<sup>[a]</sup> Hannover University, Institute of Organic Chemistry, Schneiderberg 1B, 30167 Hannover, Germany  
Fax: (internat.) +49-(0)511/762-4616  
E-mail: duddeck@mbox.oci.uni-hannover.de

<sup>[b]</sup> Institute of Organic Catalysis Research at Rostock University, Buchbinderstr. 5–6, 18055 Rostock, Germany

<sup>[c]</sup> S. V. Lebedev Central Synthetic Rubber Research Institute, Gapsalskaya 1, St. Petersburg 198035, Russia

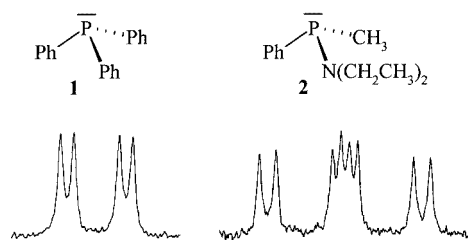
<sup>[d]</sup> Centre of Molecular and Macromolecular Studies, Polish Academy of Sciences, Department of Organic Sulfur Compounds, 90–363 Łódź, Sienkiewicza 112, Poland

Although the <sup>103</sup>Rh nucleus has some advantageous properties (spin 1/2 and 100% natural abundance), it is not easy to monitor by direct <sup>103</sup>Rh NMR measurement because of its low receptivity (18% of that of <sup>13</sup>C) and rather long spin-lattice relaxation times.<sup>[4–6]</sup> So far, only one study has reported the <sup>103</sup>Rh chemical shift for the bis(trimethylphosphite) adduct of dirhodium tetraacetate (δ = 6694 ppm).<sup>[7]</sup> In our dirhodium system, however, any direct <sup>103</sup>Rh NMR spectroscopy is impossible due to the relatively low solubility of **Rh\*** in CDCl<sub>3</sub>.

## Results and Discussion

Very recently, we reported the “dirhodium method” as the first to discriminate enantiomeric phosphane sulfides (R<sub>3</sub>P=S) in a direct way; as for any other previously studied ligand,<sup>[1]</sup> the adducts (Scheme 1) are kinetically unstable.<sup>[8]</sup> However, when we later turned to phosphanes (R<sub>3</sub>P) as ligands we were surprised to find that phosphane adducts are kinetically stable, i.e., the lifetimes of these adducts are long with respect to the NMR timescale. Thus, for the first time we were able to see the [**Rh\***←phosphane] adducts in the ambient temperature <sup>31</sup>P NMR spectra without any averaging; the <sup>31</sup>P signals are doublets of doublets due to one- and two-bond <sup>103</sup>Rh couplings (adducts with **1**, see Scheme 2 and Table 1 and Table 2). In the case of chiral phosphanes, such as **2**, a further doubling of the signal is caused by diastereomeric dispersion.

For the first time in our dirhodium project, this offers the possibility of indirect <sup>103</sup>Rh observation by <sup>31</sup>P-detected <sup>103</sup>Rh HMQC NMR experiments. Experiments of this kind — or analogous <sup>1</sup>H-detected <sup>103</sup>Rh HMQC — have not been described very frequently as they require special equipment.<sup>[5,6,9]</sup> Furthermore, it was thought that if more



Scheme 2. Structures of the phosphanes **1** and **2** (2 as racemate) and the respective  $^{31}\text{P}$  signals; for the  $^{103}\text{Rh}$ ,  $^{31}\text{P}$  coupling constants in **1** and **2** and for the dispersion  $\Delta\nu$  in **2** see Tables 1 and 2

Table 1.  $^1\text{H}$ ,  $^{13}\text{C}$ ,  $^{31}\text{P}$ , and  $^{103}\text{Rh}$  chemical shifts ( $\delta$ , in ppm), coupling constants  $^nJ(^{31}\text{P}, \text{X})$  of free  $\text{PPh}_3$  (**1**) and of the adduct  $\text{Rh}^* \leftarrow \text{1}$  (1:1 molar ratio of the components), adduct formation shifts ( $\Delta\delta$ , in ppm); in  $\text{CDCl}_3$

X	Free ligand			Ligand in the adduct		
	$\delta$	$^nJ(^{31}\text{P},\text{X})$	$\delta$	$^nJ(^{31}\text{P},\text{X})$	$\Delta\delta$	
$^1\text{H}$	<i>ortho</i>	7.35	n.d. <sup>[a]</sup>	7.59	$^3J = 10.7$	$\approx 0.3$
	<i>meta</i>	to	n.d.	$\approx 7.23$	n.d.	$-0.1$ to $0$
	<i>para</i>	7.28	n.d.	7.42	$^5J = 0-2$	$\approx 0.1$
$^{13}\text{C}$	<i>ipso</i>	137.3	$^1J = 10.8$	130.2	$^1J = 33.4$	$-7.1$
	<i>ortho</i>	133.7	$^2J = 19.4$	134.4	$^2J = 10.6$	$-2.6$
	<i>meta</i>	128.5	$^3J = 7.0$	128.9	$^3J = 9.8$	$0.2$
	<i>para</i>	128.7	$^4J \leq 1$	130.6	$^4J \leq 3$	$1.9$
$^{31}\text{P}$		$-4.2$		$-35.3$	$^1J_{\text{RhP}} = 96.1$ $^2J_{\text{RhP}} = 23.3$	$-31.1$
$^{103}\text{Rh}$	(1)		6963			
	(2)		7455			

[a] n.d.: not determined due to signal overlap or signal complexity.

than one such insensitive nucleus (e.g.,  $^{103}\text{Rh}$ ) is coupled to the sensitive detection nucleus ( $^1\text{H}$  or  $^{31}\text{P}$ ), triple-quantum effects may modulate the intensities and even the positions of the cross-peaks because all of the involved nuclei are ubiquitous (100% natural abundance) and rules valid for simple AX spin systems might not be applicable.<sup>[10,11]</sup> Therefore, we first had to explore the correct parameters in the HMQC experiment for our first-order AMX spin system ( $A = ^{31}\text{P}$ ; M and X =  $^{103}\text{Rh}$ ). This is described in the Appendix.

### $^{31}\text{P}$ -Detected $^{103}\text{Rh}$ HMQC NMR Spectroscopy

Despite the low solubility of the complexes, we succeeded in obtaining  $^{103}\text{Rh}$  correlation signals by  $^{31}\text{P}$ -detected HMQC spectroscopy (Figure 1 and 2). The choice of the transfer delay  $d_2$  according to Equations (7) and (8) (see Appendix) allows the discrimination and selection of signals originating from Rh(1) or Rh(2). Using the coupling constants  $^nJ(^{103}\text{Rh}, ^{31}\text{P})$  for the complex  $[\text{Rh}(2)-\text{Rh}(1) \leftarrow \text{1}]$  (Figure 1), we obtained a first maximum for Rh(1) at  $d_2 = 5$  ms,  $f_1(0.005) = 0.940$ , while Rh(2) cannot be observed:  $f_2(0.005) = 0.024$ . The reverse situation occurs at  $d_2 = 21$  ms,  $f_1(0.021) = 0.002$ ,  $f_2(0.021) = 0.990$ , thus only a correlation signal for Rh(2) is observable. These predictions were verified experimentally. As exemplified in Figure 1, the choice of other delays allows the simultaneous observation

Table 2.  $^1\text{H}$ ,  $^{13}\text{C}$ ,  $^{31}\text{P}$ , and  $^{103}\text{Rh}$  chemical shifts ( $\delta$ ), coupling constants  $^nJ(^{31}\text{P}, \text{X})$  of free  $\text{rac-Ph-P}(\text{CH}_3)\text{-N}(\text{CH}_2\text{-CH}_3)_2$  (**2**) and of the adduct  $\text{Rh}^* \leftarrow \text{2}$  (1:1 molar ratio of the components), adduct formation shifts ( $\Delta\delta$ , in ppm), and dispersion effects ( $\Delta\nu$ , in Hz, at 11.74 Tesla); in  $\text{CDCl}_3$

X		Free ligand <sup>[a]</sup>		Ligand in the adduct <sup>[a]</sup>		$\Delta\delta$	$\Delta\nu$
		$\delta$	$^nJ(^{31}\text{P}, \text{X})$	$\delta$	$^nJ(^{31}\text{P}, \text{X})$		
$^1\text{H}$	P-CH <sub>3</sub>	1.489	$^2J = 5.6$	1.985	$^2J = 9.7$	0.50	1.7
	N-CH <sub>2</sub>	3.023	$^3J = 9.7$	3.301	$^3J = 9.2$	0.28	< 1
		2.999		3.282			
	N-CH <sub>2</sub> -CH <sub>3</sub>	1.078	$^4J \leq 0.5$	1.084	$^4J \leq 0.5$	0.006	< 1
	ortho	7.370	$^3J \approx 10$	7.789	$^3J \approx 9$	0.42	$\approx 9$
				7.773		0.40	
$^{13}\text{C}$	meta	7.322	$^4J \approx 2$	7.23	n.d. <sup>[b]</sup>	n.d.	n.d.
	para	7.226	$^5J < 1$	7.353	$^5J \approx 1$	0.16	$\approx 1$
	P-CH <sub>3</sub>	14.1	$^1J = 18.2$	11.6	$^1J = 17.8$	-2.5	72.6
				11.1	$^1J = 15.6$	-3.0	
	N-CH <sub>2</sub>	43.7	$^2J = 14.6$	41.8	$^2J = 2-3$	-1.9	28.4
				41.6	$^2J = 2-3$	-2.1	
	N-CH <sub>2</sub> -CH <sub>3</sub>	15.2	$^3J = 3.1$	14.5	$^3J = 3.1$	-0.7	18.2
				14.4	$^3J = 3.1$	-0.8	
	ipso	144.5	$^1J = 14.6$	134.6	$^1J = 34.8$	9.9	25.9
				134.4	$^1J = 36.7$	10.1	
	ortho	129.5	$^2J = 16.1$	131.3	$^2J = 10.3$	1.8	0.9
				131.2	$^2J = 10.3$	1.7	
$^{31}\text{P}$	meta	128.0	$^3J = 4.1$	128.3	$^3J = 9.6$	0.3	5.2
				128.3	$^3J = 9.4$	0.3	
	para	127.2	$^4J = 1.0$	130.0	$^4J = 2.4$	2.8	2.5
				130.0	$^4J = 2.6$	2.8	
		49.9		11.5	$^1J_{\text{RhP}} = 106.2$ $^2J_{\text{RhP}} = 21.5$	-38.4	89.1 <sup>[c]</sup>
				11.0	$^1J_{\text{RhP}} = 106.2$ $^2J_{\text{RhP}} = 23.0$	-38.9	
$^{103}\text{Rh}$	(1)	—		6949, 6963			182 <sup>[c]</sup>
	(2)	—		7153			9 <sup>[c]</sup>

[a] Dispersions at MTPA-OCH<sub>3</sub>:  $^1\text{H}$ :  $\delta = 2.99$  and  $2.97$  ppm,  $\Delta\nu = 12.1$  Hz;  $^{13}\text{C}$ :  $\delta = 54.6_0$  and  $54.5_6$  ppm,  $\Delta\nu = 4.0$  Hz. [b] n.d.: not determined due to signal overlap or signal complexity. [c] At 9.4 Tesla.

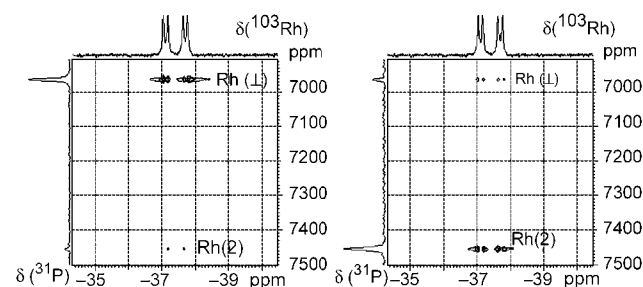


Figure 1.  $^{31}\text{P}$ ,  $^{103}\text{Rh}\{^1\text{H}\}$  HMQC NMR spectra of  $[\text{Rh}^* \leftarrow \text{1}]$  at ca. 298 K, magnitude representation; left: transfer delay  $d_2 = 2.6$  ms, selection of Rh(1):  $f_1(0.0026) = 0.692$ ,  $f_2(0.0026) = 0.125$ ; right: transfer delay  $d_2 = 11.6$  ms, selection of Rh(2):  $f_1(0.0116) = -0.234$ ,  $f_2(0.0116) = -0.671$ ; calculated from  $J_1 = 95.5$ ,  $J_2 = 21.7$  Hz

of both signals, although with a somewhat reduced intensity.

In the  $F_2$  dimension ( $^{31}\text{P}$ ), the signals appear as doublets, split by the coupling constants  $^1J(^{103}\text{Rh}, ^{31}\text{P})$  and  $^2J(^{103}\text{Rh}, ^{31}\text{P})$ , as expected. An additional splitting of ca 10 Hz is observed in the  $F_1$  dimension ( $^{103}\text{Rh}$ ), provided

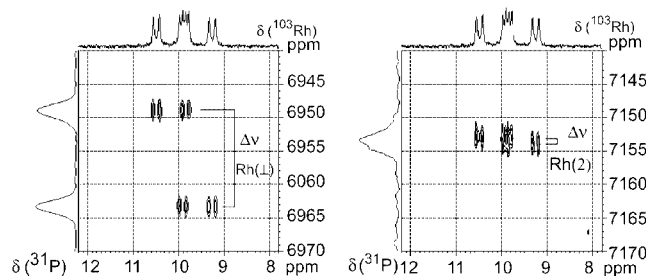


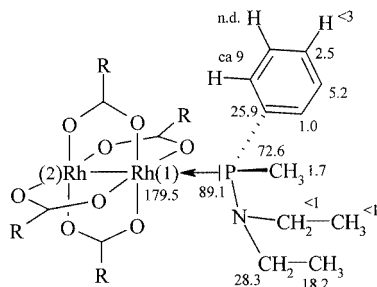
Figure 2. Sections of  $^{31}\text{P}$ - $^{103}\text{Rh}\{^1\text{H}\}$  HMQC NMR spectra of  $[\text{Rh}^* \leftarrow \mathbf{2}]$  at ca. 298 K; digital resolution in  $F_1$  is 2.9 Hz per point; top: transfer delay  $d_2 = 4.5$  ms, selection of Rh(1):  $f_1(0.0045) = 0.95$ ,  $f_2(0.0045) = 0.02$ ; bottom: transfer delay  $d_2 = 19.0$  ms, selection of Rh(2):  $f_1(0.019) = -0.001$ ,  $f_2(0.019) = 0.967$ ; calculated from  $J_1 = 105.2$ ,  $J_2 = 22.0$  Hz

the digital resolution is sufficient. We attribute this to the homonuclear coupling  $^1J(^{103}\text{Rh}, ^{103}\text{Rh})$  which is to be regarded as a “passive coupling” with respect to the  $^{31}\text{P}$ ,  $^{103}\text{Rh}$  spin pair under observation and should show up in  $F_1$ . For the related symmetric phosphite adduct  $[\text{Rh}_2(\mu\text{-OAc})_4]\text{-}[\text{P}(\text{OMe})_3]_2$  this coupling was determined to be 8 Hz.<sup>[7]</sup> Another origin for this splitting is unlikely as the protons are decoupled and a coupling to the fluorine atoms is not observable: the  $^{19}\text{F}\{^1\text{H}\}$  NMR signal of ( $\text{Rh}^* \leftarrow \mathbf{1}$ ) is a singlet at  $\delta = -72$  ppm with a half-width of 3 Hz (including 1 Hz line broadening by exponential multiplication).

### $^1\text{H}$ , $^{13}\text{C}$ , $^{31}\text{P}$ , and $^{103}\text{Rh}$ NMR Parameters of $\mathbf{1}$ and $\mathbf{2}$ and Chiral Recognition

All chemical shifts and coupling constants of the phosphanes  $\mathbf{1}$  and  $\mathbf{2}$ , as free ligands and as their adducts with  $\text{Rh}^*$ , are listed in Table 1 and Table 2. In addition, the complexation shifts  $[\Delta\delta = \delta(\text{adduct}) - \delta(\text{free})]$  are given, and Table 2 shows the dispersion effects  $\Delta v$  (in Hz), which are the signal splittings due to the existence of two diastereomeric complexes. Dispersion values are field-dependent and refer to  $B_0 = 11.74$  Tesla corresponding to 500 MHz  $^1\text{H}$  (except for the  $^{103}\text{Rh}$  values:  $B_0 = 9.4$  Tesla, see Scheme 3).

Strong complexation shifts  $\Delta\delta$  are observed for the phosphorus atom and for carbons nearby, and numerous  $^{31}\text{P}$ ,  $^1\text{H}$  and  $^{31}\text{P}$ ,  $^{13}\text{C}$  coupling constants are changed significantly as well, up to threefold or down to one half. This is clearly



Scheme 3. Diastereomerism dispersions ( $\Delta v$ , in Hz) of  $\text{Rh}^* \leftarrow \mathbf{2}$ , in  $\text{CDCl}_3$  at 11.74 Tesla ( $^{103}\text{Rh}$  at 9.4 Tesla);  $\text{R} = \text{MTPA}$ ; the two ethyl groups are not diastereotopic due to rapid interchange by nitrogen inversion; in contrast, the hydrogen atoms of the  $\text{CH}_2$  groups are diastereotopic

a consequence of the above-mentioned strong interaction between the phosphanes and the rhodium atoms they are ligated to. Even a deshielding of 3.2 ppm for the *para*-carbon in  $\mathbf{2}$  and one of 1.9 ppm for  $\mathbf{1}$  can be noticed indicating that the inductive effect of the phosphorus atom on the benzene system is severely changed by adduct formation.

As can be seen in Scheme 3, strong dispersions appear at the phosphorus and the carbon atoms of  $\mathbf{2}$ . Thus, enough nuclei exist for a safe, direct determination of the enantiomeric ratio of the phosphane (chiral recognition). Interestingly, the  $^1\text{H}$  atoms in the phosphane do not show well-resolved signals in these phosphanes, except for the  $\text{P-CH}_3$  signal — although this nucleus is generally favourable for chiral recognition — and measurements of further nuclei are often not required.<sup>[1,8]</sup> Currently, we are investigating a great variety of further chiral phosphanes to see whether or not this is a general rule.

It should be noted that dispersions of  $\text{Rh}^*$  signals can be observed in the phosphane adducts with  $\mathbf{2}$  as well, namely those of the  $^1\text{H}$  and the  $^{13}\text{C}$  signal of the methoxy group in the MTPA ligands ( $^1\text{H}$ :  $\delta = 2.99$  and  $2.97$  ppm,  $\Delta v = 12.1$  Hz;  $^{13}\text{C}$ :  $\delta = 54.6_0$  and  $54.5_6$  ppm,  $\Delta v = 4.0$  Hz). This is another proof for the fact that the adducts  $\text{Rh}^* \leftarrow \mathbf{1}$  and  $\text{Rh}^* \leftarrow \mathbf{2}$  are kinetically stable. If the complexes were kinetically unstable (as usually occurs for ligands other than phosphanes), only one time-averaged signal each would be visible.

As mentioned above,  $^{103}\text{Rh}$  NMR spectroscopy is not straightforward. Only a few reports seem to exist approaching stereochemical problems by  $^{103}\text{Rh}$  NMR spectroscopy, all on mononuclear complexes. They cover studies on catalytically active species, for example on diastereomeric enamide complexes,<sup>[12]</sup> on the stereoselectivity of the hydrogen addition to them,<sup>[13]</sup> or on the relation between  $\delta(^{103}\text{Rh})$  and changes in the ligand sphere affecting catalytic activity.<sup>[9f,9j]</sup>

In our study, the rhodium atoms reflect the diastereomerism of the  $\text{Rh}^* \leftarrow \mathbf{2}$  adducts (Figure 2). The directly attached rhodium atom  $[\text{Rh}(1)]$  shows a large chemical shift difference of 14 ppm for the two diastereomeric complexes, corresponding to a dispersion ( $\Delta v$ ) of 182 Hz whereas, expectedly, the remote one  $[\text{Rh}(2)]$  is much less sensitive; the correlation peaks can show a slight dispersion of 9 Hz, whereas the  $^{103}\text{Rh}$  signal in the  $F_1$  projection cannot resolve it (Figure 2, right). This proves the sensitivity of the rhodium nuclei in the chiral recognition experiment. Further molecular systems are currently under investigation in our laboratory.

### Conclusion

For the first time, a methodology was derived for observing  $^{103}\text{Rh}$  resonances in dirhodium-phosphane adducts (AMX spin systems) based on  $^{31}\text{P}$ -detected  $^{103}\text{Rh}$  HMQC NMR spectroscopy. It is shown that not only  $^{31}\text{P}$  and  $^{13}\text{C}$  but also  $^{103}\text{Rh}$  signals reflect the stereochemistry of the complexes with chiral phosphanes with great sensitivity.

## Experimental Section

**Compounds:** The synthesis of **Rh\*** has been described before.<sup>[1a]</sup> Triphenylphosphane (**1**) is commercially available. *N,N*-Diethylamino-(methyl)(phenyl)phosphane (**2**) was synthesized according to a known procedure: Bis(*N,N*-diethylamino)phenylphosphane [**PhP**(NEt<sub>2</sub>)<sub>2</sub>], prepared from dichloro(phenyl)phosphane and diethylamine,<sup>[14]</sup> was reacted with dichlorophenylphosphane as described<sup>[15]</sup> (although without solvent) to produce *N,N*-diethylamino-(chloro)(phenyl)phosphane [**PhP**(NEt<sub>2</sub>)Cl]. This compound was converted into **2** by reaction with MeLi in diethyl ether according to the procedure described by Nöth et al.<sup>[16]</sup> Yield 74%.

**NMR Spectroscopy:** <sup>1</sup>H (500.1 MHz), <sup>13</sup>C (125.8 MHz), and <sup>31</sup>P NMR measurements (202.4 MHz) of the free ligands **1** and **2** in the absence and presence of **Rh\*** were performed on a Bruker DRX-500 spectrometer equipped with a broad-band probe head. Solutions were about 0.05–0.06 M in CDCl<sub>3</sub>. Standards were internal tetramethylsilane ( $\delta = 0$ ) for <sup>1</sup>H and <sup>13</sup>C, and external aqueous H<sub>3</sub>PO<sub>4</sub> (85%) ( $\delta = 0$ ) for <sup>31</sup>P. Digital resolutions were 0.27 Hz/point in the <sup>1</sup>H, 0.48 Hz/point in the <sup>13</sup>C and 0.43 Hz/point in the <sup>31</sup>P NMR spectra. <sup>19</sup>F NMR (235.4 MHz) of [**Rh\***←**1**] was measured on a Bruker AC 250 spectrometer with the shift referenced against CCl<sub>3</sub>F.

Typically, the samples were prepared by mixing 48.6 mg of **Rh\*** (0.043 mmol) and a molar equivalent of **1** in 0.75 mL CDCl<sub>3</sub>; 7  $\mu$ L (1 drop) of [D<sub>6</sub>]acetone were added to increase the solubility of **Rh\***.<sup>[1c,8]</sup>

The unequivocal signal assignments in the <sup>1</sup>H and <sup>13</sup>C NMR spectra of **1** and **2** were assisted by H,H COSY, and <sup>1</sup>H-detected <sup>13</sup>C HMQC and HMBC NMR experiments using standard Bruker software. In cases where signal splittings due to <sup>31</sup>P-coupling had to be differentiated from dispersion effects ( $\Delta\nu$ ), spectra were recorded at different B<sub>0</sub> (9.40 and 11.74 Tesla). ( $\Delta\nu$  values are field-dependent, coupling constants are not.)

<sup>103</sup>Rh NMR spectroscopy was carried out on a Bruker ARX 400 spectrometer, equipped with a commercial triple-resonance probe, by “inverse detection” with <sup>31</sup>P as the sensitive nucleus. The standard four-pulse HMQC sequence with continuous proton decoupling was applied,<sup>[17,18]</sup> the choice of the transfer delay ( $d_2$ ) was according to criteria described in the text. The chemical shifts were referenced against  $\Xi$  (<sup>103</sup>Rh) = 3.16 MHz.<sup>[19]</sup> The samples of both complexes had a tetramethylsilane proton frequency of 400.130010 MHz, leading to a rhodium reference frequency,  $\delta(^{103}\text{Rh}) = 0$ , of 12.644108 MHz. Each experiment was performed at least twice with a variation of the rhodium offset and the  $t_1$  increment to ensure that the signals in the  $F_1$  dimension (<sup>103</sup>Rh) are not folded. The digital resolution in this direction was better than 0.5 ppm in the final spectra that were recorded for shift determination. Rhodium shifts were reproducible to within  $\pm 2$  ppm; we attribute observed variations to slight temperature changes (rhodium shifts have a pronounced temperature coefficient<sup>[9c][19b]</sup>). Although the data were acquired with TPPI phase cycling, a proper phasing of the signals was not always possible (regardless of whether an additional refocusing delay of duration  $d_2$  was inserted between the last HF pulse and the data acquisition or not), hence some spectra presented in this paper are in the magnitude mode.

For a given spin system, the effect of varying experimental parameters on the HMQC spectra was tested by simulation with the NMR- $\text{SIM}$  program (Bruker Rheinstetten). In all cases, results were as predicted by Equations (1)–(9) (see Appendix), and they were compatible with the experimental results.

## APPENDIX

**Signal Intensities and Multiple-Quantum Coherences in HMQC Spectroscopy of First-Order AMX Spin Systems (A = <sup>31</sup>P; M and X = <sup>103</sup>Rh):** The following discussion holds for the standard four-pulse HMQC experiment,  $\pi/2(^{31}\text{P}) - d_2 - \pi/2(^{103}\text{Rh}) - d_0/2 - \pi(^{31}\text{P}) - d_0/2 - \pi/2(^{103}\text{Rh})$  – acquisition<sup>[17]</sup> in its simple as well as in its phase-sensitive (TPPI) version. The behaviour of the three-spin system <sup>31</sup>P-<sup>103</sup>Rh(1)-<sup>103</sup>Rh(2) with  $J[\text{P,Rh}(1)] = J_1$  and  $J[\text{P,Rh}(2)] = J_2$  under the influence of this sequence can be described as follows. At the beginning of the evolution period  $d_0$ , just after the first  $\pi/2(^{103}\text{Rh})$  pulse ( $t = d_2$ ), the state of the three-spin system is given by the density operator:

$$\sigma = (0Rh) + (1Rh_1) + (1Rh_2) + (2Rh) \quad (1)$$

where

$$(0Rh) = P(\pi/2)f_0(d_2) \quad (2)$$

$$(1Rh_1) = -2P(0)Rh_1(\pi/2)f_1(d_2) \quad (3)$$

$$(1Rh_2) = -2P(0)Rh_2(\pi/2)f_2(d_2) \quad (4)$$

$$(2Rh) = -4P(\pi/2)Rh_1(\pi/2)Rh_2(\pi/2)f_{12}(d_2) \quad (5)$$

with

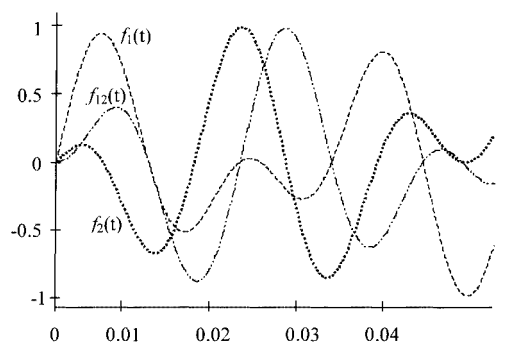
$$f_0(t) = \cos(\pi J_1 t) \cos(\pi J_2 t) \quad (6)$$

$$f_1(t) = \sin(\pi J_1 t) \cos(\pi J_2 t) \quad (7)$$

$$f_2(t) = \cos(\pi J_1 t) \sin(\pi J_2 t) \quad (8)$$

$$f_{12}(t) = \sin(\pi J_1 t) \sin(\pi J_2 t) \quad (9)$$

The <sup>31</sup>P chemical shift frequency is set to zero in these equations, and the notation follows that given in ref.:<sup>[11]</sup>  $P(\varphi)$  and  $Rh_i(\varphi)$  denote the phosphorus and rhodium,  $Rh(i)$ , spin operators for arbitrary phase  $\varphi$ . The zero- and two-spin rhodium coherences ( $0Rh$ ) and ( $2Rh$ ) are suppressed by complete phase cycling. The single-rhodium terms ( $1Rh_1$ ) and ( $1Rh_2$ ) produce the desired 2D peaks at true rhodium chemical shifts in the  $F_1$  dimension. The magnitude of these correlation signals is defined by the trigonometric factors  $f_1(t)$  and  $f_2(t)$ , see Equations (7) and (8) and Scheme 3. It is important to note that the extreme points of  $f_1(t)$  and  $f_2(t)$  do not coincide with the extreme points of  $\sin(\pi J_1 t)$  and  $\sin(\pi J_2 t)$ . They cannot be deduced from the equation  $d_2 = (2J)^{-1}$ , as is normal for HMQC, as this might lead to complete lack of signal intensity in unfavourable cases (see Scheme 4)! A homonuclear coupling between the rhodium atoms would lead to a splitting along  $F_1$  by  $J(\text{Rh,Rh})$  solely of the ( $1Rh$ ) correlation signals. This has been tested by simulation (see Exp. Sect.).



Scheme 4. Time dependence of the trigonometric factors  $f_n(t)$  [Equations (7)–(9)] in a three-spin system <sup>31</sup>P-<sup>103</sup>Rh-<sup>103</sup>Rh, calculated for  $J_1 = 95.5$  Hz and  $J_2 = 21.6$  Hz (values applicable for [**Rh\***←**1**])



## Acknowledgments

This work has been performed within the project "Biologically Active Natural Products: Synthetic Diversity" (Department of Chemistry, Hannover University) and was supported by the Deutsche Forschungsgemeinschaft and the German Academic Exchange Service (DAAD). J. O. is grateful to the Alexander-von-Humboldt foundation for a fellowship.

- [1] [1a] K. Wypchlo, H. Duddeck, *Tetrahedron: Asymmetry* **1994**, 5, 27. [1b] K. Wypchlo, H. Duddeck, *Chirality* **1997**, 9, 601. [1c] S. Hameed, R. Ahmad, H. Duddeck, *Heteroatom Chem.* **1998**, 9, 471. [1d] S. Hameed, R. Ahmad, H. Duddeck, *Magn. Reson. Chem.* **1998**, 36, S47. [1e] C. Meyer, H. Duddeck, *Magn. Reson. Chem.* **2000**, 38, 29; see also: C. Meyer, PhD thesis, Hannover University, **1999**.
- [2] It has been shown that enantiomeric purities of aromatic functionalities can be determined by  $^{31}\text{P}$  NMR spectroscopy using a mononuclear bdpp-containing rhodium complex: J. M. Buriak, J. A. Osborn, *J. Chem. Soc., Chem. Commun.* **1995**, 689.
- [3] [3a] G. R. Sullivan, *Top. Stereochem.* **1978**, 10, 287. [3b] P. L. Rinaldi, *Progr. NMR Spectrosc.* **1983**, 15, 291. [3c] D. Parker, *Chem. Rev.* **1991**, 91, 1441.
- [4] C. Brevard, P. Granger, *Handbook of High Resolution Multinuclear NMR*, John Wiley & Sons, Toronto **1981**, p. 158.
- [5] B. E. Mann, in *Transition Metal Nuclear Magnetic Resonance* (Ed.: P. S. Pregosin), Elsevier Science Publishers, Amsterdam **1991**, p. 177ff.
- [6] W. v. Philipsborn, *Chem. Soc. Rev.* **1999**, 28, 95.
- [7] E. B. Boyar, S. D. Robinson, *Inorg. Chim. Acta* **1982**, 64, L193.
- [8] S. Rockitt, H. Duddeck, J. Omelanczuk, *Chirality* **2001**, 13, 214.
- [9] Some examples: [9a] C. Brevard, R. Schimpf, *J. Magn. Reson.* **1982**, 47, 528. [9b] C. J. Elsevier, J. M. Ernsting, W. G. J. de Lange, *J. Chem. Soc., Chem. Commun.* **1989**, 585. [9c] J. M. Ernsting, C. J. Elsevier, W. G. J. de Lange, K. Timmer, *Magn. Reson. Chem.* **1991**, 29, S118. [9d] C. J. Elsevier, B. Kowall, H. Kragten, *Inorg. Chem.* **1995**, 34, 4836. [9e] L. Carlton, *Magn. Reson. Chem.* **1997**, 35, 153. [9f] K. Angermund, W. Baumann, E. Dinjus, R. Fornika, H. Görls, M. Kessler, C. Krüger, W. Leitner, F. Lutz, *Chem. Eur. J.* **1997**, 3, 755. [9g] N. Feiken, P. Pregosin, G. Trabesinger, *Organometallics* **1998**, 17, 4510. [9h] J. G. Donkervoort, M. Bühl, J. M. Ernsting, C. J. Elsevier, *Eur. J. Inorg. Chem.* **1999**, 27. [9i] M. Bühl, W. Baumann, R. Kadyrov, A. Börner, *Helv. Chim. Acta* **1999**, 82, 811. [9j] W. Leitner, M. Bühl, R. Fornika, C. Six, W. Baumann, E. Dinjus, M. Kessler, C. Krüger, A. Ruffinska, *Organometallics* **1999**, 18, 1196.
- [10] [10a] D. Nanz, W. von Philipsborn, *J. Magn. Reson.* **1991**, 92, 560. [10b] H. Rüegger, D. Moskau, *Magn. Reson. Chem.* **1991**, 29, S11.
- [11] B. T. Heaton, J. A. Iggo, I. S. Podkorytov, D. J. Smawfield, S. P. Tunik, R. Whyman, *J. Chem. Soc., Dalton Trans.* **1999**, 1917.
- [12] T. Ohkuma, R. Noyori, *Chemtracts: Org. Chem.* **1993**, 6, 325.
- [13] B. R. Bender, M. Koller, D. Nanz, W. von Philipsborn, *J. Am. Chem. Soc.* **1993**, 115, 5889.
- [14] G. Ewart, D. S. Payne, A. L. Porte, A. P. Lane (in part), *J. Chem. Soc.* **1962**, 3984.
- [15] N. A. Andreev, O. N. Grishina, *Zh. Obshch. Khim.* **1979**, 49, 2230, engl. Transl. 1959.
- [16] H. Nöth, H.-J. Vetter, *Chem. Ber.* **1963**, 96, 1109.
- [17] A. Bax, R. H. Griffey, B. L. Hawkins, *J. Magn. Reson.* **1983**, 55, 301.
- [18] [18a] R. Benn, C. Brevard, *J. Am. Chem. Soc.* **1986**, 108, 5622. [18b] R. Benn, A. Ruffinska, *Magn. Reson. Chem.* **1988**, 26, 895.
- [19] [19a] R. G. Kidd, R. J. Goodfellow, in *NMR and the Periodic Table* (Eds.: R. K. Harris, B. E. Mann), Academic Press, London **1978**, Chap. 8. [19b] R. J. Goodfellow, in *Multinuclear NMR* (Ed.: J. Mason), Plenum Press, New York **1987**, chapter 20.

Received April 22, 2002

[I02208]